

The Contrast-to-Noise Ratio for Image Quality Evaluation in Scanning Electron Microscopy

F. TIMISCHL

JEOL Technics Ltd., 2-6-38 Musashino, Akishima-shi, Tokyo, Japan

Summary: The contrast-to-noise ratio (CNR) is presented and characterized as a tool for quantitative noise measurement of scanning electron microscope (SEM) images. Analogies as well as differences between the CNR and the widely used signal-to-noise ratio (SNR) are analytically and experimentally investigated. With respect to practical SEM image evaluation using the contrast-to-noise ratio, a standard specimen and an evaluation program are presented. SCANNING 37:54–62, 2015. © 2014 Wiley Periodicals, Inc.

Key words: scanning electron microscopy, contrast, noise, contrast-to-noise ratio, image evaluation

Introduction

Evaluation of scanning electron microscope (SEM) image quality is of major importance in the instrument's development process as well as for the end user. Image quality consists of multiple factors, such as noise, resolution, and the electrical or mechanical stability of the instrument.

Several approaches have been made to unify these parameters into a single one (Joy *et al.*, 2010; Wang and Bovik, 2002), which can provide a mean for overall assessment of the image quality achieved by a certain instrument.

On the other hand, separate evaluation of different image quality related parameters is an important tool within the instrument's development process or for trouble shooting purposes.

The present work is an attempt to provide and characterize a useful approach to measurement of noise in SEM images using the contrast-to-noise ratio (CNR). While the CNR has been extensively used in medical imaging (Bechara *et al.*, 2012), noise measurement in SEM imaging is still dominated by the signal-to-noise ratio (SNR) (Marturi *et al.*, 2012; Tileli *et al.*, 2009; Baumann and Reimer, '81; Oho and Suzuki, 2011). Although a basic introduction of the CNR in SEM imaging can be found in Sato *et al.* (2011), no analytical approach has been provided yet to characterize the CNR with respect to the SNR.

Based on a suitable definition of the CNR, this paper shows the equivalence in basic information content of the CNR and the SNR, and points out differences between both with respect to practical use in SEM image evaluation.

CNR evaluation of SEM images is experimentally demonstrated using both a standard specimen and an evaluation program optimized with respect to compositional contrast.

Materials and Methods

The proposed image evaluation program is implemented using the free software numerical computational package Scilab 5.4.1. Images for experimental evaluation are obtained using a JEOL JSM-IT300 SEM (Tokyo), which employs a thermionic tungsten emitter.

Results and Discussion

Definition

The objective is to provide a measure for statistical noise in SEM images. Noise is always correlated to the amount of useful information, and therefore cannot be evaluated on its own; it always has to be related to the

Address for reprints: F. Timischl, JEOL Technics Ltd., 2-6-38 Musashino, Akishima-shi, Tokyo 196-0021, Japan.
E-mail: ftimisch@jeol.co.jp

Received 3 September 2014; Accepted with revision 31 October 2014

DOI: 10.1002/sca.21179

Published online 22 December 2014 in Wiley Online Library
(wileyonlinelibrary.com).

signal or contrast in the image under consideration (Marturi *et al.*, 2012). Since the desired information in SEM images is rather contrast than the signal itself, we refer image contrast to image noise and use the CNR as a quantitative and qualitative measure of image noise as follows (Sato *et al.*, 2011).

$$\text{CNR} = \frac{\text{Contrast}}{\text{Noise}} = \frac{|\mu_1 - \mu_2|}{\sqrt{\sigma_1^2 + \sigma_2^2}} \quad (1)$$

μ_1 , μ_2 , σ_1 and σ_2 in Equation (1) are the expectation values and standard deviations of two different signals (e.g. two areas of different brightness in the same SEM image). The above definition of CNR has been employed in medical imaging (Bechara *et al.*, 2012). We use this definition because of its simplicity, its applicability to images obtained with standard specimens, and its independence of image adjustment parameters as shown below¹.

Other methods for numerical measurement of contrast such as the Michelson contrast or Weber contrast measure signal difference normalized to an averaged or uniform background in order to account for the adaption of visual perception to the background (Thompson, 2011). Because of the sequential signal acquisition process in a SEM and the fact that signals and signal differences of a SEM image can be arbitrarily shifted (while preserving absolute signal differences) using the brightness adjustment function, we use a contrast definition omitting normalization to background in the present work.

The above definition requires an image providing at least two areas that are distinctly distinguishable from each other. It has to be noted that contrast $|\mu_1 - \mu_2|$ can refer to any type of contrast, such as material contrast, topographic contrast, voltage contrast and others. In principle, any specimen providing at least two distinguishable areas of this type is suited for CNR evaluation.

In the present work, we focus on CNR evaluation with respect to material contrast, and propose the specimen shown in Figure 1(a) as a standard specimen for CNR evaluation. In order to eliminate topographic and charging contrast effects, we propose a polished carbon block half coated with gold, thus providing a flat surface containing two areas of different atomic composition. This specimen allows CNR evaluation with respect to compositional contrast, arising from backscattered electrons, secondary electrons or both (Walker, 2008). Figure 1(b) shows a SEM image of the specimen in Figure 1(a) using a conventional Everhart–Thornley (ET) type secondary electron detector under defocused

condition to avoid influence of surface contamination or remaining topographic contrast².

The parameters of Equation (1) can be obtained graphically from the image histogram in Figure 1(c) immediately. $|\mu_1 - \mu_2|$ is given by the horizontal offset of the two signal peaks. Under the assumption that the central limit theorem holds, the signal peaks in Figure 1(c) can be approximated to have Gaussian distribution, and σ_1 and σ_2 can therefore be obtained by

$$\text{FWHM} = 2\sqrt{2 \cdot \ln(2)} \cdot \sigma \approx 2.35 \cdot \sigma, \quad (2)$$

where FWHM is the full width at half signal height of each signal peak (Timischl, 2011).

The numerical approach to obtain values for the parameters used in Equation (1) is to approximate μ_1 and μ_2 by the sample mean m , and σ_1 and σ_2 by the sample standard deviation s for each signal.

$$m = \frac{1}{N} \sum_{i=1}^N x_i \quad (3)$$

$$s = \sqrt{\frac{1}{N-1} \sum_{i=1}^N (x_i - m)^2} \quad (4)$$

x_i denotes the pixel values (i.e. the pixel luminance), and N is the number of pixels in each area.

In contrast to the CNR described above, the widely used SNR is defined by

$$\text{SNR} = \frac{\text{Signal}}{\text{Noise}} = \frac{\mu}{\sigma} \quad (5)$$

where μ and σ are the signal value and the standard deviation of a single signal (or signal peak) in the SEM image. However, different from Equation (1), μ in Equation (5) is not simply the location of the signal peak in the image histogram, it is the relative position of the signal peak from an offset value (for example with the beam current set to zero), which is not necessarily equal to the origin of the abscissa. Presuming that the numerator of Equation (5) is the difference between signal and offset, and that the offset signal contains no noise, it becomes evident that SNR and CNR have basically equivalent information content.

Properties of Image Histograms

The number of detected electrons per pixel under given observation conditions depends on the specimen composition (the secondary electron yield), and is

¹ $\sigma_1^2 + \sigma_2^2$ in Equation (1) can be divided by 2 in order to comply with the conventional definition of root mean square (rms). Since the factor 1/2 does not have any qualitative influence on the discussion below, it is omitted for the sake for simplicity.

² All SEM images shown in this work are 8-bit images. The presented concept however does not change with bit depth and is universally applicable.

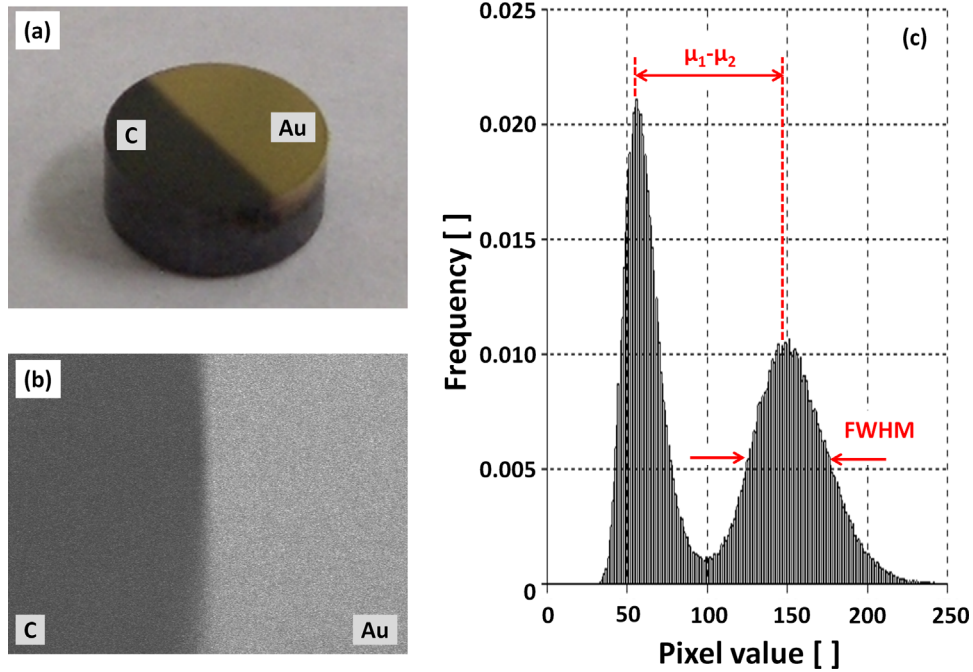


Fig. 1. (a) The proposed standard specimen for CNR evaluation providing two distinguishable areas, (b) a secondary electron image of the proposed standard specimen, and (c) the histogram of the image in (b).

therefore higher for Au than for C, if the standard specimen of Figure 1(a) is used. Since secondary electron emission can be assumed to be Poisson distributed, this implies higher variability (due to $\sigma = \sqrt{\mu}$) for the pixel values in the Au-region than for the C-region. The fact that the Au-peak in Figure 1(c) has a higher FWHM than the C-peak is a direct consequence of this property.

Before proceeding to actual CNR acquisition, we schematically explain how image histograms change with image contrast and brightness adjustment (Fig. 2). We assume a SEM image of a homogenous specimen

surface and thus a single image histogram peak. The area below the histogram's envelope curve is defined by the number of pixels in the image or the corresponding image area. Contrast and brightness adjustment both are assumed to affect the detector signal at latter stages in the signal transfer path. Contrast changes cause both the ideal signal (the mean of the histogram peak) as well as the noise (all other luminance values around the mean) to be amplified by a specific constant. Increasing contrast therefore shifts a stretched version of the original histogram peak to the right. Since the number of pixels does not change, the peak height decreases. Brightness changes simply add an offset to the original signal, thus shifting the histogram peak as it is to the right or left.

Acquisition and Interpretation of CNR

The following examples show how the CNR can be easily visualized and interpreted using image histograms. Figures 3(a) and (b) show two images obtained at different probe currents (30 pA for image (a) and 80 pA for image (b)), while all other observation conditions are held constant (10 kV acceleration voltage, 100 times magnification, 10 mm working distance, ET-secondary electron detector, 640 × 480 pixels, 320 ns pixel dwell time). The histogram of both images is shown in Figure 3(c), where the black histogram corresponds to image (a) and the red histogram to image (b). Using the implemented contrast and brightness adjustment

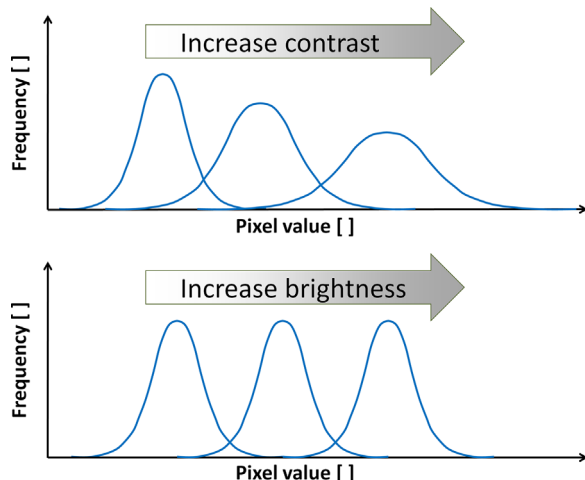


Fig. 2. Image histogram changes in case of contrast and brightness adjustment.

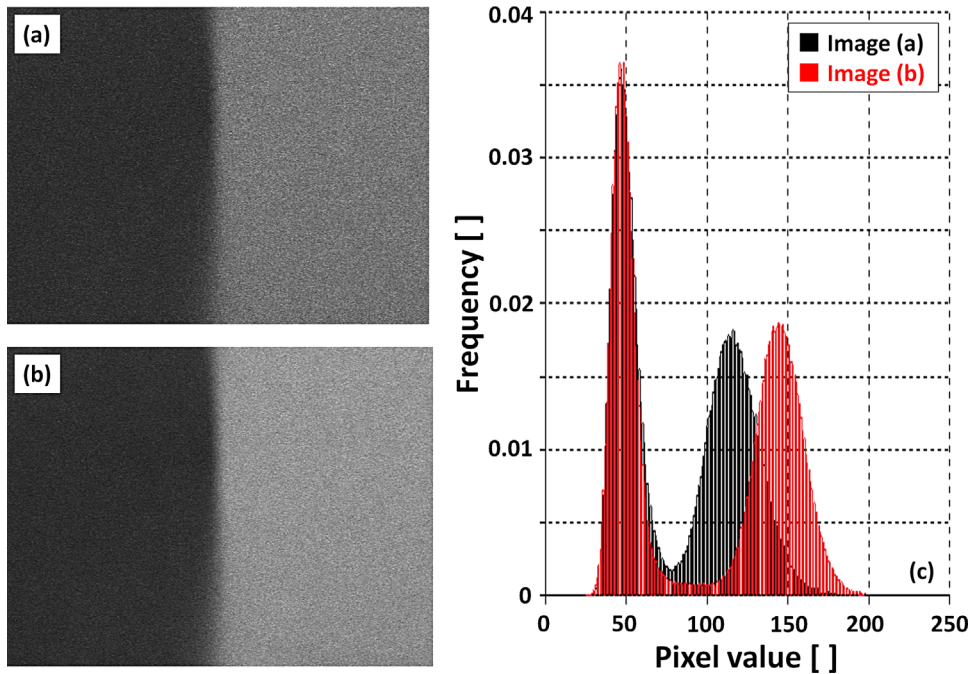


Fig. 3. Secondary electron images of the standard specimen in Figure 1(a), with probe current 30pA (a) and 80pA (b), and the histograms (c) of both images, where the dark peak of image (b) is adjusted to perfectly overlap with the dark peak of image (a).

functions of the used instrument, image (b) was adjusted so that its left histogram peak (the “dark” peak) perfectly overlaps with the corresponding peak of image (a), i.e. so that the dark peaks of both images are at the same location, and have the same peak height and FWHM. Under this condition the right peak (the “bright” peak) of image (b) shifts to the right compared to image (a) which means that image (b) has more contrast (wider distance between the peaks) under the condition of equal noise (perfectly overlapping dark peak), i.e. higher CNR than image (a).

Figure 4 shows an analogous example at equal observation conditions as described above, where the location of both histogram peaks of image (b) was adjusted to be identical to those of image (a). Under this condition, both peaks of image (a) have a wider skirt and a higher FWHM compared to those of image (b), which means that image (b) shows less noise (lower FWHM) under the condition of equal contrast (same peak distance), i.e. higher CNR than image (a).

The above examples reveal that contrast and brightness adjustment of SEM images allows almost arbitrary changes of the absolute value and noise of one signal (one “color”) in a SEM image. As a result, quantitative noise evaluation is not possible using uniform images of a single color. This is the reason why SNR evaluation requires acquisition of two images (one image for the signal and one for the offset), while CNR evaluation can be done from two different colors contained in one single image.

The offset dependence of the SNR introduces another practical problem. Decreasing image brightness shifts the image and offset peak in the histogram to the left,

while maintaining an almost constant peak distance (or contrast) between them. This works as long as the offset has a pixel value higher than zero. Further brightness decrease leads to saturation of the offset value and corrupts the relation between signal and offset, which results in wrong SNR values.

The CNR is insensitive to this problem as long as both signal peaks do not saturate, which can easily be confirmed during the process of image acquisition.

Sensitivity of CNR to Contrast and Brightness Adjustment

The examples above show how the CNR can be obtained and compared for different images, which is a common case in the hardware development process when for instance different detector setups are evaluated. As a matter of course, absolute CNR measurement requires standardized physical observation conditions (such as primary beam current, acceleration voltage, or the detector’s collector voltage). The question that is answered here is, whether the instrument’s contrast and brightness settings are excluded from this requirement.

This is of great importance considering practical utility. First, a contrast and brightness independent CNR value allows image evaluation at arbitrary conditions, i.e. the histogram “peak matching” of Figure 3(c) and Figure 4(c) does not have to be performed for actual CNR measurement. Additionally, any confinements on

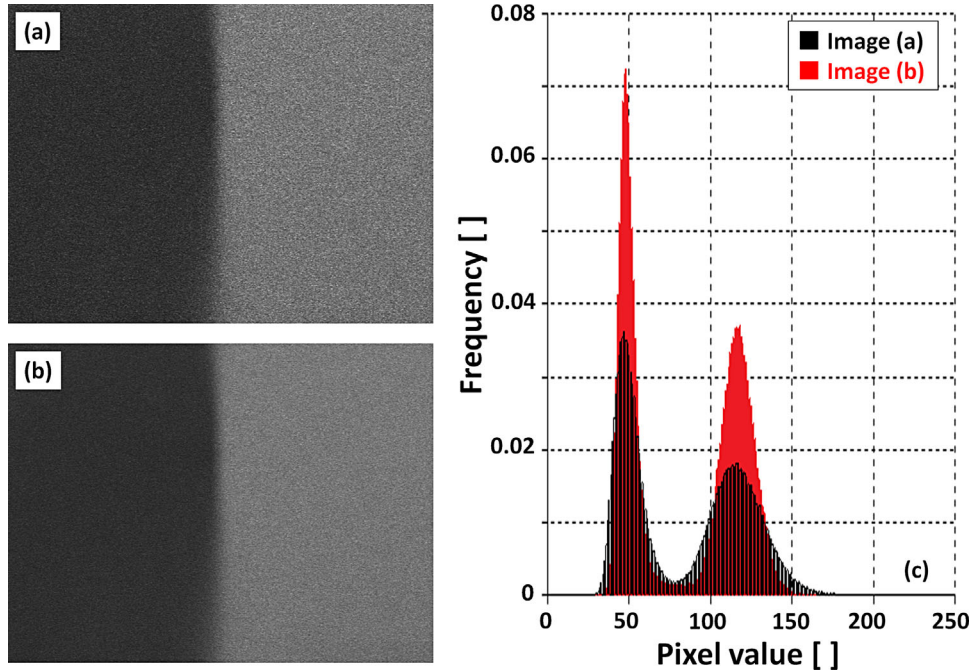


Fig. 4. Secondary electron images of the standard specimen in Figure 1(a), with probe current 30pA (a) and 80pA (b), and the histograms (c) of both images, where the location of both peaks is adjusted to match for both conditions (a) and (b).

the contrast and brightness values can lead to image saturation, which gives useless histograms and makes CNR evaluation impossible.

Assuming linearity of brightness and contrast adjustment and denoting the image adjustment parameters brightness by a and contrast by b , the signal and standard deviation after image adjustment, μ^* and σ^* , are given as follows³.

$$\mu^* = a + b \cdot \mu \quad (6)$$

$$\sigma^{*2} = b^2 \cdot \sigma^2 \quad (7)$$

a and b are constant factors, while μ^* , μ , σ^* and σ are random variables. Equation (6) and (7) hold for any signal distribution, and are therefore independent of the type of signal (secondary or backscattered electrons). Calculating the CNR after image adjustment, CNR^* gives

$$\begin{aligned} CNR^* &= \frac{(a + b \cdot \mu_1) - (a + b \cdot \mu_2)}{\sqrt{b^2 \cdot \sigma_1^2 + b^2 \cdot \sigma_2^2}} \\ &= \frac{b \cdot \mu_1 - b \cdot \mu_2}{b \sqrt{\sigma_1^2 + \sigma_2^2}} = CNR. \end{aligned} \quad (8)$$

Analogously, the SNR after image adjustment, SNR^* is given by

$$SNR^* = \frac{a + b \cdot \mu}{b \cdot \sigma} \neq SNR. \quad (9)$$

The above derivation shows that the CNR is independent of contrast and brightness values, while the SNR depends on both parameters for the general case that $a \neq 0$. a can be set to 0 by reacquisition of the signal offset for every image to be evaluated.

Figure 5 shows a series of test images obtained with the specimen of Fig. 1(a) at 10 kV acceleration voltage, 30pA probe current, 95 times magnification, 10mm working distance, 640 × 480 pixels, and 320ns pixel dwell time, using the ET-type secondary electron detector. Physical observation conditions are held constant while contrast and brightness are adjusted as indicated. Table I shows numerical 12 bit contrast and brightness values, and CNR and SNR values obtained via the numerical approach using Equations (3) and (4). The table entries reflect the above theoretical results, namely the fact that CNR is almost independent of contrast and brightness settings (sample mean $m = 3.805$, sample standard deviation $s = 0.010\%$ of m). As explained above, the fact that the signal offset generally changes with brightness and contrast changes can lead to a saturated offset value, which corrupts the calculated SNR. Images (7)~(9) are examples of this scenario, where the calculated SNR values clearly differ from those of images (1)~(6). Accurate SNR

³It is assumed that contrast and brightness affect the detector signal at the photomultiplier (in the case of an ET type secondary electron detector) or after the preamplifier, i.e. at latter stages in the signal transfer path. In this case, contrast and brightness changes can be assumed to have negligible influence on the noise of the detector signal as shown by Timischl, (2011), which implies that noise after image adjustment can be expressed by Equation (7).

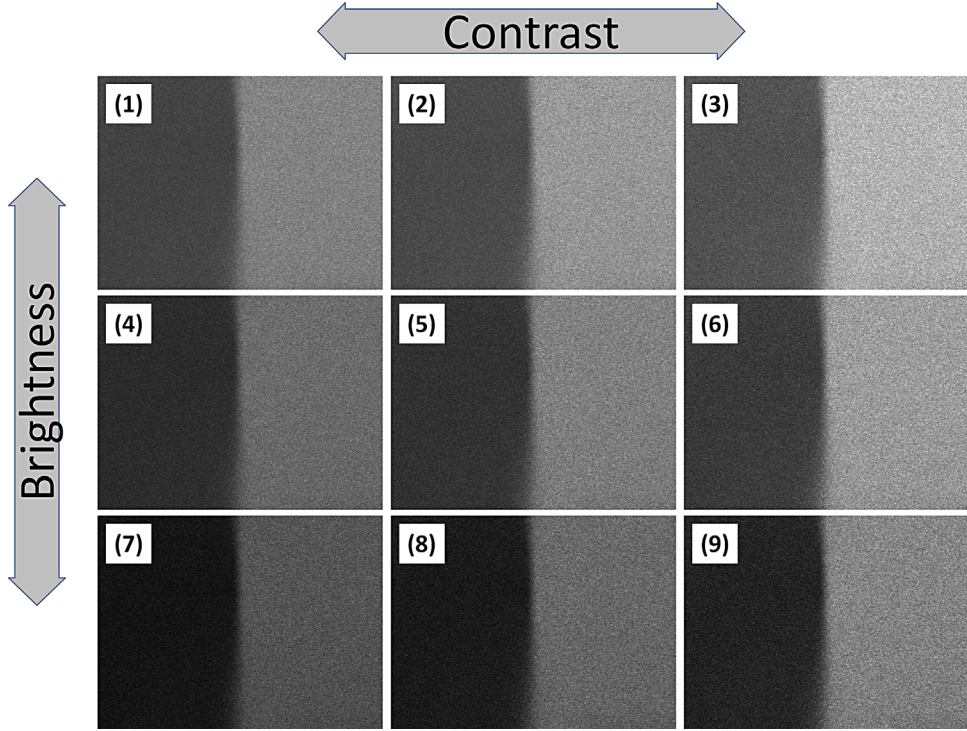


Fig. 5. Secondary electron images for CNR and SNR measurements at different contrast and brightness settings.

TABLE I Contrast and brightness 12-bit DAC values, and CNR and SNR values of the test images in Figure 5.

Image	Contrast	Brightness	CNR	SNR
1	1267	1858	3.811	3.687
2	1299	1858	3.807	3.718
3	1335	1858	3.818	3.723
4	1267	1847	3.806	3.706
5	1299	1847	3.802	3.687
6	1335	1847	3.811	3.709
7	1267	1836	3.807	3.084
8	1299	1836	3.784	3.209
9	1335	1836	3.795	3.314

measurement is not possible in these cases in contrast to CNR measurement, which is independent of the actual offset value. SNR is calculated for the dark half of the remaining images (1)~(6) giving sample mean $m = 3.705$, sample standard deviation $s = 0.414\%$ of m , where the dependency of the SNR on contrast and brightness is eliminated due to separate signal offset acquisition for every image using the beam blanking function.

CNR Evolution in the Signal Transfer Path

Timischl, (2011) showed how the SNR depends on the stage order in the signal transfer path of a SEM using a standard ET-type secondary electron detector. The fact that CNR and SNR basically have the same information content suggests that both show a very similar if not equal dependence on stage order. For verification, an analysis analogous to Timischl, (2011) is performed in the following for the CNR.

We assume a 5-stage noise model as shown in Figure 6, where [1] *Gun* denotes the generation of the primary electron beam at the electron gun and its limitation by the objective lens aperture. [2] *SE* denotes the emission of secondary electrons at the specimen and their collection by the secondary electron detector's collector. [3] *Scint* describes the scintillation process. Finally, the stages [4] *PC* and [5] *Dyn* describe the signal conversion by the photocathode of the PMT (photomultiplier tube) and the signal multiplication in the PMT. μ and σ are the expectation value and the standard deviation of each stage corresponding to the notation above. The analysis of Timischl, (2011) gives for the SNR at the last stage, $SNR_{tot(5)}$

$$SNR_{tot(5)} = \frac{1}{\left(\frac{\sigma_{GUN}^2}{\mu_{GUN}^2} + \frac{\sigma_{SE}^2}{\mu_{GUN}\mu_{SE}^2} + \frac{\sigma_{Scint}^2}{\mu_{GUN}\mu_{SE}\mu_{Scint}\mu_{Scint}^2} + \frac{\sigma_{PC}^2}{\mu_{GUN}\mu_{SE}\mu_{Scint}\mu_{PC}\mu_{PC}^2} + \frac{\sigma_{Dyn}^2}{\mu_{GUN}\mu_{SE}\mu_{Scint}\mu_{PC}\mu_{Dyn}^2} \right)^{\frac{1}{2}}} \quad (10)$$

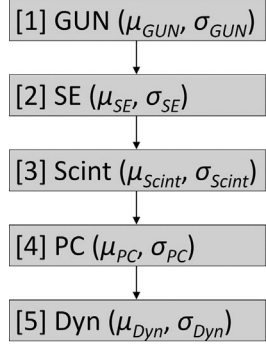


Fig. 6. The 5-stage noise model of the signal-transfer path in a SEM (Timischl, 2011).

where a uniform specimen (e.g. a polished specimen surface of uniform composition) is assumed.

Considering that the specimen used for CNR acquisition consists of two areas of different composition, we assume expectation values $\mu_{1,SE}$ and $\mu_{2,SE}$, and standard deviations $\sigma_{1,SE}$ and $\sigma_{2,SE}$ for the secondary electron emission from area 1 and 2 of the standard specimen in Figure 1(a), respectively. Following the approach of Timischl, (2011), this gives for the total expectation values $\mu_{1,tot(5)}$ and $\mu_{2,tot(5)}$ and standard deviations $\sigma_{1,tot(5)}$ and $\sigma_{2,tot(5)}$ at the fifth stage of the signal transfer path

$$\mu_{1,tot(5)} = \mu_{GUN}\mu_{1,SE}\mu_{Scint}\mu_{PC}\mu_{Dyn} \quad (11)$$

$$CNR_{tot(5)} = \frac{|1-x|}{\sqrt{1+x^2} \cdot \left[\frac{\sigma_{GUN}^2}{\mu_{GUN}^2} + \left(\frac{1}{x} \right) \left(\frac{\sigma_{SE}^2}{\mu_{GUN}\mu_{SE}^2} + \frac{\sigma_{Scint}^2}{\mu_{GUN}\mu_{SE}\mu_{Scint}^2} + \frac{\sigma_{PC}^2}{\mu_{GUN}\mu_{SE}\mu_{Scint}\mu_{PC}^2} + \frac{\sigma_{Dyn}^2}{\mu_{GUN}\mu_{SE}\mu_{Scint}\mu_{PC}\mu_{Dyn}^2} \right)^{\frac{1}{2}} \right]^{\frac{1}{2}}} \quad (17)$$

$$\mu_{2,tot(5)} = \mu_{GUN}\mu_{2,SE}\mu_{Scint}\mu_{PC}\mu_{Dyn}, \quad (12)$$

$$\begin{aligned} \sigma_{1,tot(5)} &= (\mu_{GUN}\mu_{1,SE}\mu_{Scint}\mu_{PC}\mu_{Dyn})^2 \\ &\cdot \left(\frac{\sigma_{GUN}^2}{\mu_{GUN}^2} + \frac{\sigma_{1,SE}^2}{\mu_{GUN}\mu_{1,SE}^2} \right. \\ &+ \frac{\sigma_{Scint}^2}{\mu_{GUN}\mu_{1,SE}\mu_{Scint}^2} \\ &+ \frac{\sigma_{PC}^2}{\mu_{GUN}\mu_{1,SE}\mu_{Scint}\mu_{PC}^2} \\ &\left. + \frac{\sigma_{Dyn}^2}{\mu_{GUN}\mu_{1,SE}\mu_{Scint}\mu_{PC}\mu_{Dyn}^2} \right), \end{aligned} \quad (13)$$

$$\begin{aligned} \sigma_{2,tot(5)} &= (\mu_{GUN}\mu_{2,SE}\mu_{Scint}\mu_{PC}\mu_{Dyn})^2 \\ &\cdot \left(\frac{\sigma_{GUN}^2}{\mu_{GUN}^2} + \frac{\sigma_{1,SE}^2}{\mu_{GUN}\mu_{2,SE}^2} \right. \\ &+ \frac{\sigma_{Scint}^2}{\mu_{GUN}\mu_{2,SE}\mu_{Scint}^2} \\ &+ \frac{\sigma_{PC}^2}{\mu_{GUN}\mu_{2,SE}\mu_{Scint}\mu_{PC}^2} \\ &\left. + \frac{\sigma_{Dyn}^2}{\mu_{GUN}\mu_{2,SE}\mu_{Scint}\mu_{PC}\mu_{Dyn}^2} \right). \end{aligned} \quad (14)$$

The relation between the expectation values for the secondary electron emission (i.e. the secondary electron emission coefficient) from both areas on the specimen can be expressed by

$$\mu_{2,SE} = x \cdot \mu_{1,SE}. \quad (15)$$

Thus, it follows for the corresponding standard deviations that

$$\sigma_{2,SE} = \sqrt{x} \cdot \sigma_{1,SE}, \quad (16)$$

which holds for both Poisson-distributed secondary electron emission (Sim *et al.*, 2003) and Binomial-distributed backscattered electron emission (Baumann and Reimer, '81) from the specimen.

Substitution of Equations (15) and (16) into Equations (11) ~ (14) relates the total expectation values $\mu_{1,tot(5)}$ and $\mu_{2,tot(5)}$ and standard deviations $\sigma_{1,tot(5)}$ and $\sigma_{2,tot(5)}$ at the fifth stage to each other. Substituting the result in Equation (1) finally gives

$$CNR_{tot(5)} = \frac{|1-x|}{\sqrt{1+x^2} \cdot \left[\frac{\sigma_{GUN}^2}{\mu_{GUN}^2} + \left(\frac{1}{x} \right) \left(\frac{\sigma_{SE}^2}{\mu_{GUN}\mu_{SE}^2} + \frac{\sigma_{Scint}^2}{\mu_{GUN}\mu_{SE}\mu_{Scint}^2} + \frac{\sigma_{PC}^2}{\mu_{GUN}\mu_{SE}\mu_{Scint}\mu_{PC}^2} + \frac{\sigma_{Dyn}^2}{\mu_{GUN}\mu_{SE}\mu_{Scint}\mu_{PC}\mu_{Dyn}^2} \right)^{\frac{1}{2}} \right]^{\frac{1}{2}}}. \quad (17)$$

Comparison of Equation (10) and (17) shows that $CNR_{tot(5)}$ and $SNR_{tot(5)}$ differ by the specimen dependent factor $\frac{|1-x|}{\sqrt{1+x^2}}$ which can be assumed to be constant and therefore without significance. Additionally, terms before and after the second stage, *SE* (i.e. the specimen) in the denominator of $CNR_{tot(5)}$ differ by the factor $(\frac{1}{x})$. This results from the fact that the specimen is the only remaining difference when acquiring $CNR_{tot(5)}$ and $SNR_{tot(5)}$ at equal hardware and observation conditions⁴. Depending on the choice of x (i.e. the difference of the

⁴The standard specimen of Fig. 1(a) with $\mu_{1,SE}$ and $\mu_{2,SE} = x \cdot \mu_{1,SE}$ is used for $CNR_{tot(5)}$ while $SNR_{tot(5)}$ is obtained using a uniform specimen of $\mu_{1,SE}$ (for instance one half area of the standard specimen in Fig. 1(a)).

secondary electron emission coefficient) the influence of the stages after the specimen is suppressed or enhanced if compared to the case of the SNR. $x = 1$ gives the same results as the SNR case.

However, it has to be noted that specimen dependence is not an exclusive characteristic of the CNR; it is present for the SNR in the same way since SNR and CNR use the same specimen dependent electron signal.

Assuming Poisson distribution ($\mu = \sigma^2$) and the same observation and collection conditions as given in Timischl, (2011), SNR_{tot} and CNR_{tot} can be calculated for each stage in the signal transfer path analogous to the above derivation of Equation (10) and Equation (17). Figure 7 shows this scenario, i.e. the development of SNR_{tot} and CNR_{tot} from one stage to another. For comparison purposes, CNR_{tot} and SNR_{tot} values are normalized to 100. The theoretical result shows a dramatic decrease of both CNR_{tot} and SNR_{tot} from the first to the second stage and a gradual decrease after the second stage. This is due to the fact that secondary electron yield and collection efficiency are relatively low compared to the signal conversion and amplification efficiency within and after the secondary electron detector. The first stage [1] GUN and the second stage [2] SE are therefore of major importance considering contrast and noise in the signal chain of a SEM. A more detailed discussion is given in Timischl, (2011).

Equation (17) allows calculation of a theoretical CNR and comparison with experimentally obtained values as demonstrated in the following example. Observation conditions are chosen according to the example of Table I, collection conditions as described in Timischl, (2011), and secondary electron yields $\delta_C = 0.143$ and $\delta_{Au} = 0.143$ according to Joy (2008). Using Equation (17) we obtain a theoretical value $CNR = 3.22$, which is reasonably close to the experimental value of $CNR = 3.8$ in Table I.

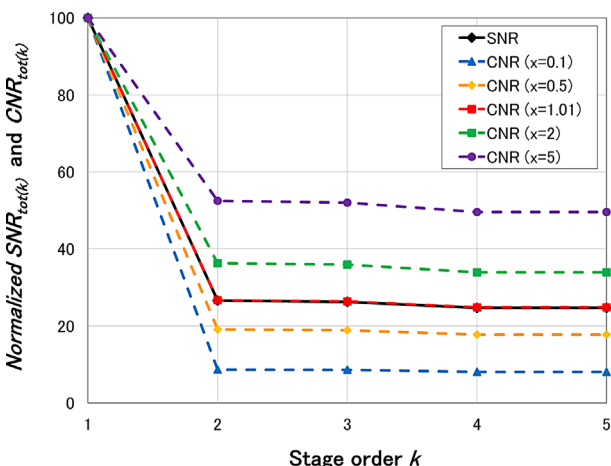
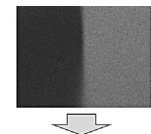
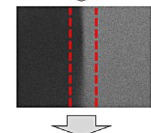


Fig. 7. $SNR_{tot(k)}$ and $CNR_{tot(k)}$ in dependence of the stage order k using realistic expectation values.

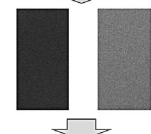
[1] Import image.



[2] Import user defined area for cutout.



[3] Divide image into two halves according to [2].



[4] Calculate sample mean and sample standard deviation for each half.

$$\mu_{Dark}, \mu_{Bright}, \sigma_{Dark}, \sigma_{Bright}$$

[5] Calculate CNR.

Fig. 8. Structure of the CNR evaluation program.

CNR evaluation program

A simple evaluation program was written in order to avoid the tedious procedure of CNR evaluation from the image histogram. Figure 8 shows the structure of the evaluation program. The evaluated image is imported, and a middle section of selectable range is cut out (to avoid the boundary region of the two specimen compositions, which might contain unwanted compositional or topographic features). The remaining image is cut in two halves, and the sample mean and sample standard deviation are computed for both halves (m_1, m_2, s_1, s_2) using Equation (3) and (4). In a last step, the CNR is computed by Equation (1).

All CNR values in this paper are obtained by use of the described evaluation program.

Discussion

At given observation conditions, contrast and noise of the SEM image are related to each other. While increasing image contrast does give higher contrast in the image, it necessarily increases image noise. CNR is suited to express this relation directly. SNR on the other hand relates noise to the physical detector signal, which can only be measured if it is referred to an offset signal.

The proposed standard specimen can be used for CNR acquisition with respect to compositional contrast. However, the concept of CNR itself, its discussed characteristics and the proposed way of acquisition are independent of the contrast type, and can therefore be applied to any other equivalent specimen that allows visualization of other contrast types.

Finally it has to be noted, that this discussion is not limited to scanning electron microscopy, but can be extended and applied to any other imaging mechanism that employs a secondary or backscattered electron signal.

Conclusion

The present work gives a discussion of the concept of CNR for evaluation of image noise in scanning electron microscopy. CNR is characterized and compared to the widely used SNR analytically and experimentally.

The major result is that both CNR and SNR allow qualitative image evaluation, and basically contain the same information content. However, CNR has several distinct advantages over SNR from the practical point of view, i.e. it requires no offset acquisition and is therefore insensitive to acquisition conditions with saturated offset values. Second, CNR is generally not influenced by contrast and brightness changes, which allows CNR acquisition under almost arbitrary observation conditions.

Because of their close relation, CNR and SNR have a very similar signal transfer characteristics.

For practical evaluation, a standard specimen allowing CNR measurement with respect to compositional contrast and an evaluation program are proposed.

References

- Baumann W, Reimer L. 1981. Comparison of the noise of different electron detection systems using a Scintillator-Photomultiplier combination. *Scanning* 4:141–151.
- Bechara B, McMahan CA, Moore WS, Noujeim M, Geha H, Teixeira FB. 2012. Contrast-to-noise ratio difference in small field of view cone beam computed tomography machines. *J Oral Science* 54:227–232.
- Joy DC. 2008. A database of electron-solid interactions. Revision # 08–1. Web address: web.utk.edu/~srcutk/database.doc.
- Joy DC, Michael J, Griffin B. 2010. Evaluating SEM Performance from the Contrast Transfer Function. *Proc. SPIE* 7638, Metrology, Inspection, and Process Control for Micro-lithography XXIV, 76383J.
- Marturi N, Dembele S, Piat N. 2012. Performance Evaluation of Scanning Electron Microscopes using Signal-to-Noise Ratio. The 8th Int. Workshop on MicroFactories, IWMF'12, Tampere. p 1–6.
- Oho E, Suzuki K. 2011. Highly accurate SNR measurement using the covariance of two SEM images with the identical view. *Scanning* 33:1–8.
- Sato M et al. 2011. Shin-Sousadenshikenbikyou [New Electron Microscopy]. Tokyo: The Japanese Society of Microscopy, Kanto Branch.
- Sim KS, Thong JTL, Phang JCH. 2003. Effect of shot noise and secondary emission noise in scanning electron microscope images. *Scanning* 26:36–40.
- Thompson W, Fleming R. 2011. Visual Perception from a Computer Graphics Perspective. Boca Raton: Taylor & Francis Group.
- Tileli V, Knowles WR, Toth M, Thiel BL. 2009. Noise characteristics of the gas ionization cascade in low vacuum scanning electron microscopy. *J Applied Physics* 106:14904–1–8.
- Timischl F, Date M, Nemoto S. 2011. A statistical model of signal-noise in scanning electron microscopy. *Scanning* 33:1–8.
- Walker CGH, El-Gomati MM, Assa'd AMD, Zadrazil M. 2008. The Secondary Electron Emission Yield for 24 Solid Elements Excited by Primary Electrons in the Range 250–5000 eV: a Theory/Experiment Comparison. *Scanning* 30: 365–380.
- Wang Z, Bovik AC., 2002. A Universal Image Quality Index. *IEEE Signal Processing Letters* 9:81–84.